Fermi Surface of Aluminum from Kohn Anomalies

JOHN W. WEYMOUTH*
Behlen Laboratory of Physics, University of Nebraska, Lincoln, Nebraska 68508
AND
R. STEDMAN
AB Atomenergi, Studsvik, Nyköping, Sweden
(Received 11 June 1970)

A careful and detailed neutron inelastic scattering measurement of the phonon-dispersion function of Al has been made along all symmetry branches and a portion of [211] L (longitudinal). The measurements were made on a three-axis spectrometer that has a double-crystal monochromator. Particular emphasis was placed on small-q increments, high relative precision in the determination of phonon frequencies, and on uniformity of conditions within runs in order to extract significant Kohn-anomaly data. Theoretical predictions on positions and relative sizes of anomalies have been compared with the observed slope curves, $\Delta\omega/\Delta q$ versus q, to yield 11 fairly certain Kohn anomalies and 8 more possible or questionable ones. Of these, 15 give Fermi-surface diameters with uncertainties of 0.5 to 1%, which are compared with the calculations of Ashcroft and of Faulkner. At least two clearly observed anomalies could not be assigned by any simple argument.

I. INTRODUCTION

The theoretical basis for the appearance of an image of the Fermi surface in phonon dispersion curves of metals via the electron-phonon interaction, originally pointed out by Kohn,[1] has been extensively treated in the literature.[2–5] The first experimental confirmation by Brockhouse *et al.*[6] of these Kohn anomalies in the dispersion curves of lead, measured with neutron inelastic scattering, has been followed by several reports of anomalies in other metals. Woods and Chen[7] and Powell, Martel, and Woods[8] measured the dispersion relations of Mo and Mo–Nb alloys and noted some anomalies which were related to calculated Fermi surfaces. In an analysis of the alloy system Pb-Bi-Ti, Ng and Brockhouse[9] reported on the changes of two anomalies as a function of the electron-per-atom ratio.

In their work on the dispersion curves of aluminum, Stedman and Nilsson[10] examined the usefulness of Kohn-anomaly observations as an analytical tool in the mapping of the Fermi surface. Since the anomalies were not large, they found it necessary to examine the slopes of the dispersion curves in order to find those points where the slope became anomalous. They assigned at least seven anomalies to points on the Fermi surface. This work was followed by Stedman *et al.*[11] in which the authors made a more extensive analysis of Kohn anomalies relative to the Fermi surface of lead, again by examining carefully the slope $\Delta\omega/\Delta q$. This work included several anomalies that were interpreted as "nondiametral," that is, arising from electron transitions in k space between parallel portions of the Fermi surface that were not related by inversion through the origin. They assigned some 16 diametral and about 8 nondiametral anomalies to transitions on the Fermi surface, resulting in a fairly complete mapping of the surface.

All of the observations cited above were made with neutron inelastic scattering using a three-axis spectrometer. Walker and Egelstaff[12] recently reported on dispersion surfaces throughout the Brillouin zone of Mo measured with neutrons and a time-of-flight method. They subtracted frequencies obtained by a Born–von Karman model calculation from the data and related the remaining anomalous regions in the zone to calculated Kohn-anomaly surfaces (or Kohn surfaces). In a similar treatment Sharp[12a] examined the discrepancies between model calculations and measured frequencies in Nb and related these to Kohn surfaces derived from Fermi-surface calculations.

Aside from the anomalies measured with neutrons, there exist in the literature only two cases of observations with thermal diffuse x-ray scattering (TDS). Paskin and Weiss[13] measured the total TDS along several symmetry directions in Pb and noted the existence of three or four anomalies. The interpretation in terms of Kohn anomalies is complicated by the competing effect of trace amounts of surface oxides. Costello and Weymouth[14] reported a TDS measurement in Cr interpreted as a Kohn anomaly in the antiferromagnetic state and which vanishes in the paramagnetic state.

The purpose of the work described here was twofold: to examine further the use of Kohn anomalies obtained from neutron inelastic scattering as a tool for the study of a Fermi surface, and to extend the measurements of Stedman and Nilsson[10] on Al. In this work the phonon measurements were designed from the beginning with the aim of locating Kohn anomalies. Thus the errors involved in obtaining frequencies from measured phonon peaks were analyzed and the precision improved. A finer q increment was used and consistency of conditions within a run was maintained. Emphasis was placed on transverse branches where favorable focusing conditions yield better precision, and the low-frequency regions of the longitudinal branches where the anomalies should be larger. Most of the data were obtained at 80°K. We have measured phonons along seven symmetry branches and have identified 11 anomalies

TABLE I. Positions and sizes of Kohn anomalies (KA) phonon wave vector $q = |\mathbf{q}|$; **G** given by one reciprocal-lattice vector of symmetry related set; electron transition $Q = |\mathbf{q}+\mathbf{G}|$; relative size estimated from factor PM/ω and given by small (S), medium (M), and large (L); sign given where fairly obvious; diam means diametral transition; ND indicates insufficient or no data. All dimensions in units of $2\pi/a$.

	Predictions							Observations and assignments			
KA No.				Size			Diam		Size		
	q	G	Q	L	T	Sign	?	q	L	T	Remarks
	[111] Branch										
1	0.07	0	0.07	L	···				ND	ND	
2	0.13	111	1.86	L	···	+			?		Suggestion in L at 0.9
3	0.23	200	2.14	M	L			0.21±0.015	+S	+L	Possible in L at 0.20
4	0.31	200	2.19	M	M			0.31±0.02		−M	Or +M in L at 0.30?
5	0.34	111	2.07	S	···						
6	0.40	200	2.26	M	M	+	yes	0.37±0.01		+L	Not seen in L
7	0.52	111	2.25	S	···	+	yes	0.495±0.02	+L		
8	0.62	0	0.62	S	···				ND		
9	0.72	$0\bar{2}\bar{2}$	2.28	S	M	−	yes	0.75±0.015	ND	−M	
	[100] Branch										
10	0.04	111	1.76	L	L				ND	ND	Possible in L at 0.07
11	0.15	111	1.82	L	L			0.18±0.01		+M	
12	0.13	200	2.13	L	···	+					
13	0.15	0	0.15	L	···						
14	0.13	0	0.13	L	···						
15	0.22	111	1.87	L	···	+					
16	0.22	200	2.22	M	···	−					
17	0.26	200	2.26	M	···	+	yes	0.24±0.01		+M	
18	0.32	0	0.32	M	···						
19	0.37	111	1.97	M	M						
20	0.72	111	2.23	M	S						
21	0.76	111	2.26	M	S	+	yes	0.78±0.01	+M?	+L	+M at (0.82±0.04) L
22	0.85	$\bar{2}00$	1.15	M	M	−	yes	0.85±0.01	?	−S	
		$\bar{2}\bar{2}0$	2.31								
23	0.89	$\bar{1}11$	1.42	VS	M						
24	0.93	0	0.93	S	S	+	yes	0.96(?)	ND	S	
		020	2.21								

TABLE I (*Continued*)

KA No.	Predictions q	G	Q	L	Size T_1 ⟨001⟩	T_2 ⟨1̄10⟩	Sign	Diam ?	Observations and assignments q	L	Size T_1	T_2	Remarks
	[110] Branch												
25	0.16	111	1.86	L	L		+			ND	ND		
26	0.12	0	0.12	L	···	···				ND			
27	0.19	111	1.89	L	M	···				−?			
28	0.28	111	1.97	M	M	···							
29	0.34	200	2.25	M	···	M	+	yes	0.34±0.02	+S		+M?	+M in T_2 at 0.30
30	0.47	111	2.13	M	S	···							
31	0.48	$\bar{2}\bar{2}0$	2.25	S	···	···	−	yes	0.57±0.02	−S?			
32	0.64	$\bar{2}\bar{2}0$	2.19	S	···	···							
33	0.61	111	2.26	M	S	···	+	yes	0.62±0.01	+L	+S		+S in T_1 at 0.60
34	0.74	$\bar{1}\bar{1}\bar{1}$	1.21	S	M	···							
									0.79	+S?	+S?		
35	0.74	$\bar{2}\bar{2}0$	2.09	S	···	···	−						
36	0.91	0	0.91	S	M	···	+	yes	0.91	−M			KA has wrong sign
		002	2.20										
37	0.86	$\bar{1}\bar{1}\bar{1}$	1.14	VS	M	···			0.83		+S		
38	1.03	0	1.03	S	···					−M?			
39	1.15	0	1.15	M	S	···	+	yes	1.15±0.01	−M			
		002	2.31						1.18±0.02		−M		
	[211] Branch												
40	0.30	200	2.25	S	T-not estimated		+	yes	0.28±0.01	+M			

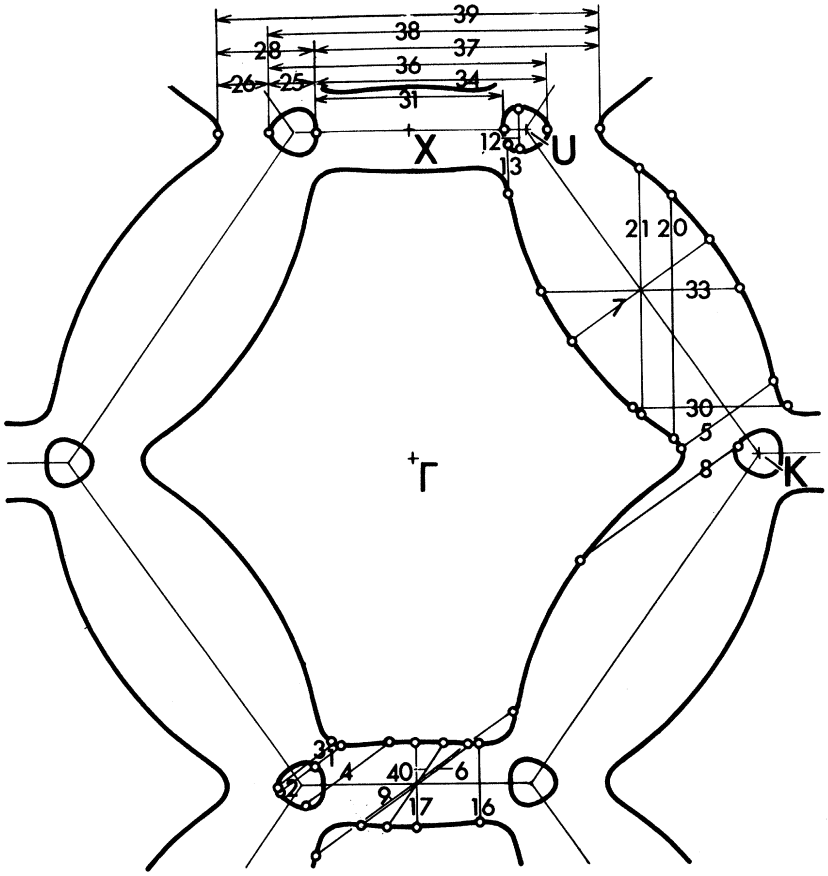

FIG. 1. A [110] section of the Al Fermi surface with predicted Kohn-anomaly transitions.

with some degree of certainty, about 8 more that are possible and about 10 more that are faintly suggested. Seven of the better anomalies are diametral, giving Fermi surface diameters with a precision of less than 1% and eight more giving possible diameters. We have also observed some anomalies that we could not assign to the Fermi surface by any simple argument.

II. KOHN ANOMALIES AND FERMI SURFACE

A. Estimation of Size

The theoretical argument for the existence of Kohn anomalies[1] is, in brief, that the conduction electrons in a metal exhibit a $\mathbf{q}$-dependent screening response to the ionic motions associated with a phonon, and the response function or its derivative passes through a singularity when the phonon wave vector $\mathbf{q}$ connects two electron states $\mathbf{k}_1$ and $\mathbf{k}_2$ at points on the Fermi surface where tangents are parallel. This singularity is reflected in a singularity in the slope of the dispersion relation $\omega(\mathbf{q})$. If $\mathbf{Q}$ is a vector which spans the extended zone surface between parallel tangents such that $\mathbf{Q}=\mathbf{k}_2-\mathbf{k}_1$, then $\mathbf{q}=\mathbf{Q}\pm\mathbf{G}$, where $\mathbf{G}$ is a reciprocal-lattice vector which brings $\mathbf{q}$ into the first zone.

If we call the relative size of an anomaly S, we can write

$$S\simeq C(MP/\omega)F(Q)f(\mathbf{v}_1,\mathbf{v}_2).$$

The curvature factor C affects both the nature and size of the anomaly.[4,5] For instance, the singularity can range from a logarithmic singularity in $d\omega/dq$ for $Q=2k_F$ and a spherical surface, to a logarithmic singularity in ω when $\mathbf{Q}$ connects flat portions of a surface.

The multiplicity factor M, in the case of diametral transitions, is equal to the number of reciprocal-lattice vectors, including $\mathbf{G}=0$, that reduces $\mathbf{Q}$ to the same $\mathbf{q}$. In the case of nondiametral transitions, an additional weighting factor of 2 (or in some cases 4) arises because these transitions come in pairs due to inversion symmetry.

The polarization factor $P=[(\mathbf{Q}\cdot\mathbf{e})/Q]^2$ depends on the transition $\mathbf{Q}$ and the phonon polarization $\mathbf{e}$ (thus, e.g., $\mathbf{G}=0$ anomalies will not appear in transverse branches). $F(Q)$ is a form factor for the scattering event which depends on the effective potential between ions due to the electron-phonon interaction. The exact form is not known in the region around $Q=2k_F$ (see, e.g., Vosko *et al.*[2]).

The factor ω^{-1} may be considered as a combination of a factor ω^{-2} in the electron-phonon scattering cross section (see Ziman[15]) and a factor ω arising from the summation over pairs of electron states contributing to the anomaly. Finally the density of states at the surface enters in through the factor $f(v_1, v_2)$, a function of the electron velocities at the Fermi surface. When the

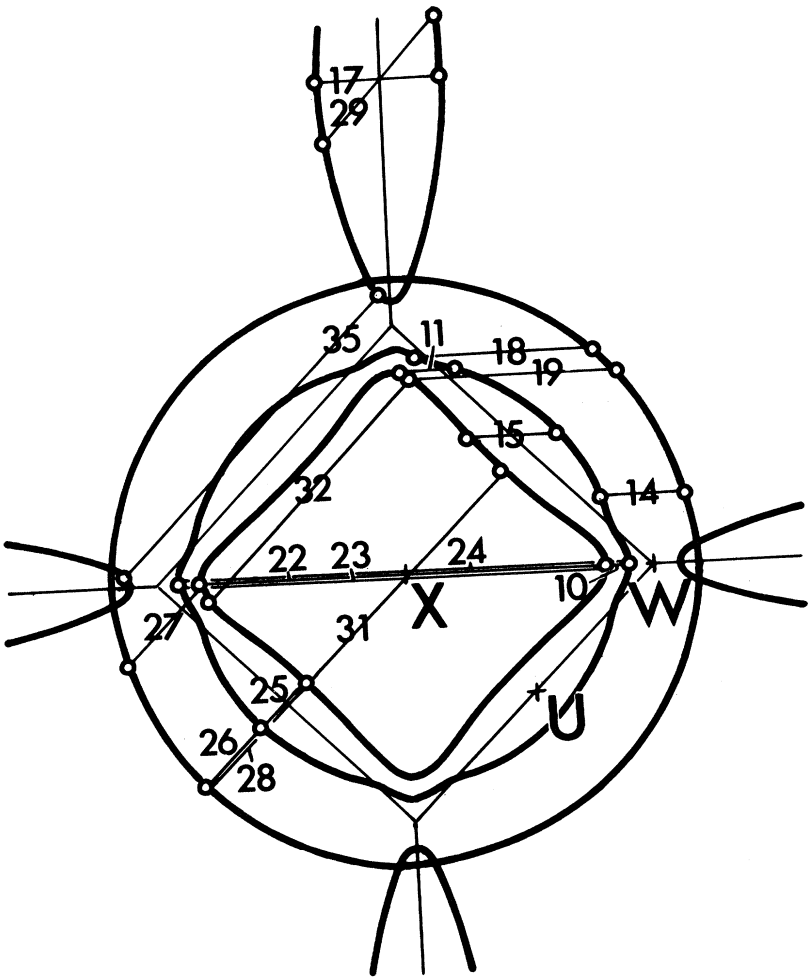

FIG. 2. A [100] section of the Al Fermi surface with predicted Kohn-anomaly transitions.

transition involves electron states near Bragg planes the situation becomes more complicated. Anomalies 25–28, 31, 32, and 34–39 are examples. The shapes of such anomalies and their relative magnitudes cannot be predicted in any simple manner. The effects described by Johnson[16] refer to this situation.

It will be seen that a complete prediction of shapes and sizes of anomalies is very difficult. Some rough estimations can be made however, of relative sizes between branches by using the factor PM/ω. These are included in Table I.

B. Aluminum Fermi Surface

The Fermi-surface model of Al which we have used is the 4-OPW (orthogonalized-plane-wave) calculation of Ashcroft[17] (designated by him as model No. 1), which he compared favorably with the de Haas–van Alphen data of Gunnersen[18] and of Larson and Gordon.[19]

We have also made comparisons of our data with the magnetoacoustic data of Kamm and Bohm[20] which in turn were compared with calculations of Segall.[21] Faulkner[22] has recently published some detailed calculations using several potentials and compared the results with the surfaces of Ashcroft and Segall, among others. Basically, the model surface is similar to a free-electron surface for three conduction electrons with a filled first zone, a second-zone hole surface centered at Γ, and a simply connected third-zone electron surface consisting of four-sided rings around the edges of the square faces of the zone. In this model there are no fourth-zone pockets. Figure 1 is a (110) section and Fig. 2 is a (100) section of this surface.

C. Geometry of Kohn Surfaces

In locating the positions of expected anomalies we used more than one approach. If one is dealing with an "empty lattice" then the Kohn surfaces are spheres of radius $2k_F$ drawn about each lattice point. The desired information is given by all the portions of these surfaces that pass through the irreducible volume of the first zone. This approximation can then be improved by rounding the surfaces where they intersect Bragg planes.

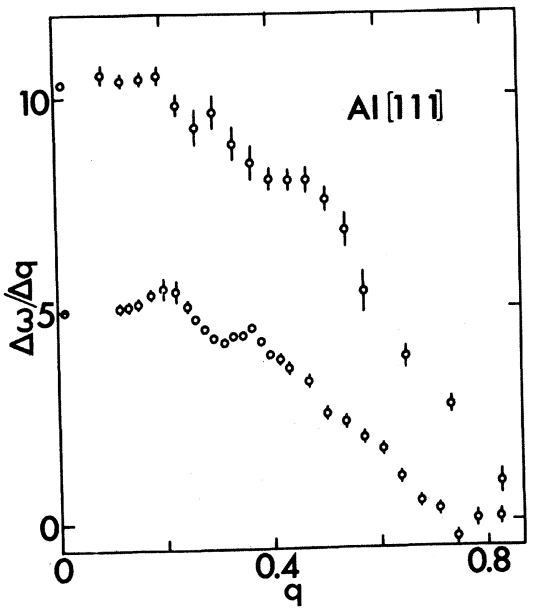

FIG. 3. Slopes $\Delta\omega/\Delta q$ versus q for the [111] branches in units of $(10^{13}$ rad/sec$)/(2\pi/a)$ versus $(2\pi/a)$. Upper curve for L branch, lower for T branch.

More specifically, one can consider the intersection of portions of the extended zone Fermi surface being used as a model with the irreducible portion of the first zone of a reciprocal space scaled to $\frac{1}{2}$ the scale of the Fermi space. This approach will yield Kohn surfaces for diametral transitions and was used to construct the diagrams in the papers by Stedman and Nilsson[10] and Stedman *et al.*[11]

Another approach is to note that the transition $\mathbf{Q}=\mathbf{k}_2-\mathbf{k}_1$ can be generated by translating the Fermi surface parallel to itself such that the surface at $\mathbf{k}_1$ is tangent to the surface at $\mathbf{k}_2$ (see Roth *et al.*[5]). By drawing extremal sections of the reduced Fermi surface in duplicate and moving one section around the edge of the other (translation with no rotation), the Kohn surface can be established by recording the locus of all the translations involved. Of course, it may be necessary to reduce $\mathbf{Q}$ to $\mathbf{q}$ by a vector $\mathbf{G}$. This latter method will give nondiametral transitions as well as diametral ones. Also, it will locate Kohn surfaces for interband transitions.

A computer calculation was made of values of $\mathbf{Q}$ for all $\mathbf{G}$ of interest and for $\mathbf{q}$ in 50 increments along [110] and [111], and 100 increments along [110] for all polarizations. This aided in the location of diametral transitions (near values of $\mathbf{q}$ where Q passed through $2k_F$) and in giving the sign of these anomalies (where Q was increasing or decreasing). This calculation also included values of the polarization factor.

Figures 1 and 2 give graphically all of the anomalies we could establish that might exist along the symmetry directions. In Table I we list these anomalies, their expected positions determined from Ashcroft's model, usually graphically, and a relative size estimation derived from the factor (PM/ω). The sign of the anomaly is given where such a determination is fairly certain. We made no estimation of the contribution from the matrix element, which might have unexpected and even drastic effects on the size, particularly near Bragg planes.

III. EXPERIMENTAL DETAILS

A. Collection of Data

All of the phonons were measured on one of the three-axis spectrometers at the *R2* reactor at Studsvik. The spectrometer described by Stedman *et al.*[23] has a double-crystal monochromator, a fixed-beam direction incident on the sample, and a stationary sample axis. High resolution and low background are achieved with these spectrometers. A typical background figure with the sample in position for a phonon measurement, but with cadmium blocking the beam from the sample to the analyzer was 7 ± 1 counts/h.

To indicate the nature of the collimation, resolution, and counting conditions encountered in these measurements, we quote some representative conditions. The following data are typical of a series of [111] T (transverse) phonons in the neighborhood of $q=0.30$. The collimation from the monochromator was 0.006 rad and that to the analyzer was 0.01 rad. A typical phonon peak, obtained with the "constant-κ" method and having ten energy increments of 0.0315×10^{13} rad/sec

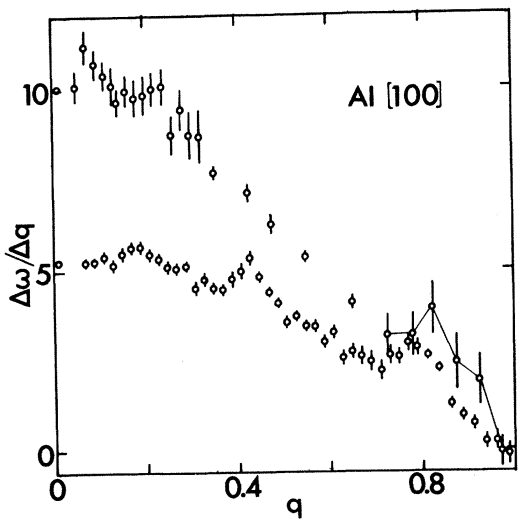

FIG. 4. Slopes $\Delta\omega/\Delta q$ versus q for the [100] branches in units of $(10^{13}$ rad/sec$)/(2\pi/a)$ versus $(2\pi/a)$. Upper curve for L branch, lower for T branch.

had a FWHM of 0.06×10^{13} rad/sec of which about 0.05×10^{13} rad/sec was instrumental resolution. The momentum resolution was 0.025 (in units of $2\pi/a$) in the [111] direction and 0.05 in both of the transverse directions $[\bar{2}11]$ and $[01\bar{1}]$. With a peak count of between 200 and 300 neutrons, these phonons were recorded in 5 to 10 h each. In Sec. III B we discuss the energy precision obtained under these and similar conditions.

In seeking Kohn anomalies the emphasis is on high relative precision, small q intervals and long unbroken runs keeping constant the analyzer Bragg angle, and beam paths. These latter conditions are, of course, necessary in order to avoid an abrupt change in focusing conditions and slight, unsuspecting changes in the absolute energy measurements which might appear as an anomaly.[24] Since the same analyzer and beam path conditions cannot be maintained throughout a branch, it is necessary to overlap a sufficient number of phonons when two runs are joined. The question of relative precisions is discussed in Sec. III B. As regards q intervals, typical increments in q are for [100], $\Delta q=0.02$ or 0.025; for [110], $\Delta q=0.02\times\sqrt{2}$ or $0.025\times\sqrt{2}$; and for [111], $\Delta q=0.01\times\sqrt{3}$ or $0.02\times\sqrt{3}$. Altogether some 260 phonons were measured.

Although the absolute value in energy is not as important as high relative precisions, the correct absolute determination in q is important since this affects the position of an anomaly. Periodic checks were made of neighboring Bragg reflections. Also the monochromatization was periodically calibrated by removing the sample, placing the analyzer in the direct, monochromatic beam and measuring the angle through which the analyzer must turn in order to diffract both left and right.

B. Analysis of Data

Since we are seeking small anomalies in the slopes of dispersion curves (typically involving sudden changes of ω of the order of 1% or less), we need to obtain $d\omega/dq$ with as high a precision as possible, compatible with other requirements. To guard against systematic errors which are functions of κ we emphasized long unbroken runs with small q intervals keeping the analyzer setting constant and keeping the same type of beam path. When the analyzer setting or beam path had to be changed in order not to depart too far from the condition of optimum resolution, runs were overlapped. In many cases measurements at 300°K corroborate the 80°K results.

In order to get as much precision as the random errors of the data allow it is not sufficient to examine visually a plotted phonon, with its error bars arising from counting statistics, and from this derive an energy and its uncertainty. A close examination of such an approach reveals that one usually overestimates the uncertainty in energy. We studied this problem and finally rejected curve fitting approaches in favor of a semiempirical relation for a central value and its uncertainty. We discuss this method at greater length elsewhere.[25] In this method the uncertainty estimations were tested against a population of simulated phonon curves generated in a computer by starting with curves of known parameters and randomizing each point with a variance equal to its size minus the background. Thus, to the extent that the starting curve for these populations resembles an experimental phonon, we have fairly accurate knowledge of the uncertainty in an experimentally derived energy. In the example cited in the previous sections, that is the [111]T phonons, some typical energy values and associated uncertainties due to counting statistics are (in units of $2\pi/a$ and 10^{13} rad/sec) $q=0.312$, $\omega=1.5634\pm0.0017$; $q=0.347$, $\omega=1.7170\pm0.0017$; $q=0.382$, $\omega=1.8805\pm0.015$. We see that in these cases the uncertainties in ω are of the order of 0.1%. This precision varied of course, depending on the focusing conditions. Values ranged from approximately 0.06 to 0.8%.

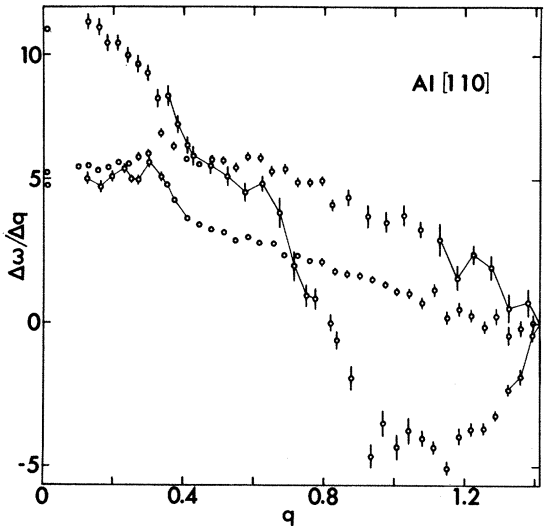

FIG. 5. Slopes $\Delta\omega/\Delta q$ versus q for the [110] branches in units of $(10^{13}$ rad/sec$)/(2\pi/a)$ versus $(2\pi/a)$. Highest curve for L branch, next highest for $T_1\langle 001\rangle$ branch, lowest for $T_2\langle\bar{1}10\rangle$ branch.

IV. RESULTS

A. Assignment of Kohn Anomalies

The results of the measurements are displayed in Figs. 3–5 where the slopes $\Delta\omega/\Delta q$ versus q are plotted for the [111], [100], and [110] branches, respectively. In making the Kohn anomaly assignments listed in Table I, we were guided by the expected values of q, the expected sign, and the relative size in the two, or three, polarization branches at the same q. In the [111] branches all anomalies are assigned. There is some

TABLE II. Diametral Kohn anomalies and Fermi-surface dimensions (all dimensions in units of $2\pi/a$).

Branch	No.	Exptl Kohn anomalies[a] q	Exptl Kohn anomalies[a] $2k_F$	Theoret q values for Kohn anomalies: Free electron[b]	Theoret q values for Kohn anomalies: Faulkner[c]	Theoret q values for Kohn anomalies: Ashcroft[d]	Exptl q values, magnetoacoustic: Kamm and Bohm[e]	Remarks: ω shift where obtainable
[111]	6	0.37±0.01	2.23±0.01	0.398	0.386±0.003		0.35±0.01	$\Delta\omega_T=(0.5\pm0.2)\%$
	7	0.49±0.02	2.23±0.02	0.522	0.525		0.50±0.06	
	9	0.75±0.02	2.26±0.02	0.756	0.770±0.003		0.78±0.02	$\Delta\omega_T=(1.3\pm0.2)\%$
[100]	17	0.24±0.01	2.24±0.01	0.255	0.246		0.23±0.03	$\Delta\omega_L\sim0.5\%$
	21	0.78±0.01	2.27±0.01	0.756	0.752±0.003			$\Delta\omega_T\sim0.2\%$
								Obs. at 0.82 in L
[110]	29	0.34±0.02	2.25±0.02	0.341	0.334±0.003			
	31	0.57±0.02	2.26±0.02	0.573	0.566±0.005	0.585		
	33	0.62±0.01	2.27±0.01	0.607	0.614±0.004		0.58±0.03	Sign wrong?
	36	0.91±0.02	2.20±0.02	1.042	0.908	0.847		Sign wrong?
	39	1.16±0.02	2.31±0.01	1.042	1.150	1.16		
[211]	40	0.28±0.01	2.23±0.01	0.305	0.288±0.004		0.27±0.03	$\Delta\omega_L=(0.5\pm0.2)\%$

[a] Data from Table I. Diameter $2k_F$ calculated from q values.
[b] Free electron $2k_F=2.255$.
[c] Reference 21 and (private communication). Uncertainty estimated when value obtained from plot.
[d] Reference 16, values taken from published plots.
[e] Reference 19, values taken from published plots.

question about the assignments of Nos. 4 and 6. The assignments of 7 and 9 fit well with the evidence.

In the [100] branches all but one of the anomalies are assigned. If the identification of $21T$ is correct, then the lack of an obvious $21L$ is disturbing. The $+M$ at $q=0.82L$, with its larger uncertainty, might be the answer. Another diametral transition, $24L$ and T may be lost, at least in L because of insufficient data. The most obvious discrepancy is the strong anomaly at $q=0.43T$ which apparently has no prediction. This is discussed below. The diametral No. 17 seems the most certain one in these branches.

In the [110] branches the assignments are the least satisfactory, with two having no clear assignments. Only one is predicted in T_1 (at $q=0.34$) which might correspond to the observed one at $q=0.30$. The most satisfactory anomalies are the diametral Nos. 29 and 33, while 31 is reasonable. Number 36 agrees well in position in the longitudinal branch but lacks a transverse contribution. Number 39 agrees well in position in two branches, but both 36 and 39 are opposite in sign to that predicted. The sign predictions are made, however, on the basis of a spherical Fermi surface, while in these cases the local deviation from a sphere is considerable. Thus it is conceivable that the curvature effect will reverse the sign. The most puzzling anomaly in these branches is at $q=0.33T$ and is discussed below.

Twelve phonons were measured along [211] L from $q=0.07$ to $q=0.34$ covering a region sufficient to yield a clear anomaly at $q=0.27$. This is identified as the diametral anomaly No. 40. No data were obtained in the T branch.

B. Fermi-Surface Dimensions

Data for the diametral anomalies are displayed in Table II along with some comparative values. The experimental values of $2k_F$ are derived from the observed values of q. The theoretical values for q are derived from the free-electron model ($2k_F=2.255$), from the values of $2k_F$ resulting from a Korringa-Kohn-Rostoker type of band-theory calculation by Faulkner[22] and, in the case of some [110] anomalies, from values derived from the diagrams in Ashcroft's paper.[17] Another set of experimental q values are taken from the published magnetoacoustic measurements of Kamm and Bohm.[20] Also included are phonon frequency shifts at anomalies where such estimations could be made.

C. Unassigned Anomalies

It has been pointed out above that some observed anomalies could not be given reasonable assignments, the worst offenders being $q=0.43$[100]T and $q=0.33$[110]T_2. A calculation by Johnson,[16] which includes the effect of off-diagonal matrix elements on the dielectric function, predicts dispersion-curve anomalies

TABLE III. Classification of anomalies according to agreement between predictions and observations. Diametral transitions indicated by D.

Fairly certain		Possible		Suggested	
$3L, 3T$		$21L$	D	$2L$	
$4T$		$29L, 29T_2$	D	$10L$	
$6T$	D	$31L$	D	$22L, 22T$	D
$7L$	D	$33L, 33T_1$	D	$24T$	D
$9T$	D	$36L$	D	$27L$	
$11T$		$39L$	D	$35L, 35T_1$	D
$17L$	D			$37T_1$	
$21T$	D			$38L$	
$39T$	D				
$40L$	D				

at these positions. Whether the observed anomalies are in fact such higher-order effects, or are normal Kohn anomalies which we failed to predict, remains an open question at this time. The problem is being examined further.

V. CONCLUSIONS

A careful and detailed measurement of the dispersion function of Al has been made along all symmetry branches and a portion of $[211]L$. An analysis of the slopes of these curves for Kohn anomalies has resulted in the fairly certain identification of 11 anomalies, 7 of these being of the diametral type. Eight more possible assignments have been made, all of these being diametral. Ten more are faintly suggested by the data. These somewhat subjective evaluations are summarized in Table III. At least three more anomalies, two of these being quite strong, are unidentified.

As regards one purpose of this experiment, it has been successful in extending the earlier measurements of Stedman and Nilsson[10] on the Fermi-surface dimensions of Al, six of the values given in that work being confirmed here with somewhat better precision. Altogether, the 14 diametral anomalies reported here give several Fermi-surface diameters with uncertainties of 0.5 to 1%. Most of these do not deviate significantly from the free-electron values, the obvious exceptions being Nos. 36 and 39 which occur where the free-electron surface has the largest amount of distortion due to energy gaps. The most consistent set of deviations from free-electron surface, which are small but possibly significant, occurs with Nos. 6, 17, and 40 which are all on the "cap" of the second zone surface and all give $2k_F$ values which are 0.5 to 1% too small. Number 29, however, is also on the cap and has no deviation from the free-electron value.

The other purpose of this experiment was to examine further the use of Kohn anomalies as a tool for the study of Fermi surfaces. Comparing the difficulty of these measurements in Al with earlier ones in Pb, we conclude that this is not a satisfactory tool in the general case, particularly when approaching a metal with little or no information about its Fermi surface. If something is known about the surface and if the electron-phonon interaction is sufficiently strong, or if the particular shape of the surface is favorable, such as large flat areas, then valuable information can be obtained. This information is complementary to such techniques as deHaas–van Alphen measurements which measure extremal areas. An advantage of Kohn anomaly determinations which might be invaluable in some cases is that a very low temperature is not required. The measurements reported in this paper were done at 80°K, while a few were repeated at 300°K.

Aside from obtaining Fermi-surface information, there is an intrinsic value in examining the electron-phonon interaction. Our experience with this experiment leads us to the conclusion that there is a good deal of information in the fine detail of dispersion curves of metals that is, as yet, untapped. So far we have been able to pay but scant attention to the relation between the theory of Kohn anomaly size and shape and the experimental evidence. No attempt has been made in this paper to examine the effect of the anomalies on phonon width, although our data contain information on this point. And finally, the existence of a few experimentally obvious but theoretically obscure anomalies is a possible indicator of much more to be explored.

ACKNOWLEDGMENTS

One of us (J.W.W.) would like to express his thanks to the Swedish Committee for Solid State Research and A. B. Atomenergi for their support and hospitality extended to him and to the University of Nebraska Research Council for a Leave-of-Absence Grant.

* Work performed at A. B. Atomenergi, Studsvik, Sweden while on leave from the Physics Department, University of Nebraska.

[1] W. Kohn, Phys. Rev. Letters **2,** 393 (1959).
[2] S. H. Vosko, R. Taylor, and G. H. Keech, Can. J. Phys. **43,** 1187 (1965).
[3] P. L. Taylor, Phys. Rev. **131,** 1995 (1963).
[4] A. M. Afanas'ev and Yu Kagan, Zh. Eksperim. i Teor. Fiz. **43,** 1456 (1962) [Soviet Phys. JETP **16,** 1030 (1963)].
[5] L. M. Roth, H. J. Zeiger, and T. A. Kaplan, Phys. Rev. **149,** 519 (1966).
[6] B. N. Brockhouse, K. R. Rao, and A. D. B. Woods, Phys. Rev. Letters **7,** 93 (1961); B. N. Brockhouse, T. Arase, G. Caglioti, K. R. Rao, and A. D. B. Woods, Phys. Rev. **128,** 1099 (1962).
[7] A. D. B. Woods and S. H. Chen, Solid State Commun. **2,** 233 (1964).
[8] B. N. Powell, P. Martel, and A. D. B. Woods, Phys. Rev. **171,** 727 (1968).
[9] S. C. Ng and B. N. Brockhouse, in *Proceedings of the Copenhagen Symposium on Inelastic Scattering of Neutrons* (International Atomic Energy Agency, Vienna. 1968), paper No. S. M. 104/53.
[10] R. Stedman and G. Nilsson, Phys. Rev. Letters **15,** 634 (1965).
[11] R. Stedman, L. Almquist, G. Nilsson, and G. Raunio, Phys. Rev. **163,** 567 (1967).
[12] C. B. Walker and P. A. Egelstaff, Phys. Rev. **177,** 111 (1969).
[12a] R. I. Sharp, J. Phys. C **2,** 432 (1969).
[13] A. Paskin and R. J. Weiss, Phys. Rev. Letters **9,** 199 (1962).
[14] J. Costello and J. W. Weymouth, Phys. Rev. **184,** 694 (1969).
[15] J. M. Ziman, *Principles of the Theory of Solids* (Cambridge U. P., Cambridge, England, 1964), p. 173.
[16] R. Johnson, Kgl. Danske Videnskab. Selskab, Matt.-Fys. Medd. (to be published); R. Johnson and A. Westin (private communication).
[17] N. W. Ashcroft, Phil. Mag. **8,** 2055 (1963).
[18] E. M. Gunnersen, Phil. Trans. Roy. Soc. London **A249,** 299 (1957).
[19] C. O. Larson and W. L. Gordon, Phys. Rev. **156,** 703 (1967).
[20] G. N. Kamm and H. V. Bohm, Phys. Rev. **131,** 111 (1963).
[21] B. Segall, Phys. Rev. **131,** 121 (1963).
[22] J. S. Faulkner, Phys. Rev. **178,** 914 (1969); additional data kindly supplied to us by J. S. Faulkner (private communication).
[23] R. Stedman, L. Almquist, G. Raunio, and G. Nilsson, Rev. Sci. Instr. **40,** 249 (1969).
[24] Although no attempt has been made in this article to analyze phonon widths obtained during these measurements, it should be noted that when measuring phonons separated by a small-q step it is possible to pass through a sharp maximum or minimum in the resolution width due to changing focusing conditions.
[25] R. Stedman and J. Weymouth, J. Phys. D **2,** 903 (1969).